International Journal of Food Sciences And Nutrition Innovations
Volume 2, Issue 1, 23-34.
e_ISSN: 3109-9025
https://e-journal.gomit.id/ijfsni
DOI : 10.58723/ijfsni.v2i1.190

Effect of Particle Size of Ophiopogon japonicus and Dioscorea opposita Meal Replacement Powder on Its in Vitro Hypoglycemic and Hypolipidemic Activities

Xue Wu
Chongqing Normal University
CHINA

Jieya Hu
Chongqing Normal University
CHINA

Ling Yang
Chongqing Normal University
CHINA

Lei Zhang*
Chongqing Normal University
CHINA

Xianlu Lei
Chongqing Normal University
CHINA

Article Info

Article history:

Received: February 30, 2026
Revised: Maret 10, 2026
Accepted: Maret 30, 2026

Keywords:

Particle Size;
Hypoglycemic Activity;
Hypolipidemic Activity;
Ophiopogon japonicus;
Dioscorea opposite.

Abstract

Background: Ophiopogon japonicus and Dioscorea opposita are prominent medicinal and edible raw materials for functional foods. In meal replacement powders, particle size is a critical factor influencing biological activities.
Aim: This study investigated the effect of particle size on the in vitro hypoglycemic and hypolipidemic functions of an O. japonicus and D. opposita meal replacement powder.
Methods: Botanical powders were prepared at 40, 60, 80, 100, and 120 mesh. Various in vitro functional indicators related to blood glucose and lipid reduction—such as glucose dialysis delay index, glucose adsorption, α-amylase inhibition, and cholesterol/sodium cholate binding capacities—were evaluated.
Result: As the crushing degree increased, all indicators initially increased and subsequently decreased. The glucose dialysis delay index and glucose adsorption capacity peaked at 100 mesh. The strongest α-amylase inhibition occurred at 80 mesh, reaching 75.48%. Additionally, cholesterol adsorption capacity, sodium cholate adsorption capacity, and sodium cholate binding capacity reached their maximum levels at 100 mesh, yielding 1.38 mg/g, 16.01 mg/g, and 69.41%, respectively.
Conclusion: Meal replacement powders processed through an 80-mesh or 100-mesh sieve possess optimal hypoglycemic and hypolipidemic potential. This study provides theoretical support for the formulation optimization of O. japonicus-D. opposita powders and serves as a processing reference for the industrial production of homologous functional foods.

To cite this article: Wu et al. (2026). Effect of Particle Size of Ophiopogon japonicus and Dioscorea opposita Meal Replacement Powder on Its in Vitro Hypoglycemic and Hypolipidemic Activities. *Journal of Food Sciences And Nutrition Innovations, 2*(1), 23-34. https://doi.org/10.58723/ijfsni.v2i1.190

INTRODUCTION

With the improvement of living standards and health awareness, people have begun to pay closer attention to the source, quality, and nutritional value of food, as well as its health-care and therapeutic functions (Sun, B. G., & Mo, Y. J. 2026). Meanwhile, the concept of medicinal and edible homology advocated by traditional Chinese medicine has gained increasing prominence and recognition in the health and wellness sector (Cheng et al. 2023). Compared with ordinary food, medicinal and edible homologous substances provide nutrition and disease prevention for humans (Wang 2023). For example, natural active ingredients such as ganoderma lucidum polysaccharides (Fu, W., & Chen, Y. 2025) , hawthorn flavonoids (Lou et al. 2025), and poria cocos triterpenoids (Gao et al. 2025) are highly valued in the health field for their excellent safety profiles, hypoglycemic and antihypertensive activities, antioxidant properties, and immune-enhancing effects. In recent years, the state has issued policies such as the Healthy China 2030 Plan Outline and the Opinions on Promoting the Inheritance, Innovation and Development of Traditional Chinese Medicine to support and encourage the development and innovation of various medicinal and edible homologous foods (Liu et al. 2022). Against this strategic backdrop, the field of medicinal and edible homologous foods

*** Corresponding author:**
Lei Zhang, Chongqing Normal University CHINA. ✉ leizhang0215@126.com

has ushered in favorable development opportunities and attracted widespread social attention (Yan et al. 2024).

Ophiopogon japonicus (mai men dong/yard lilyturf), first recorded in Shennong's Classic of Materia Medica, is a medicinal and edible herb (Zhou et al. 2025). It is rich in bioactive substances, including steroidal saponins, homoisoflavonoids, polysaccharides, amino acids, and volatile oils (Wan et al. 2023). Modern studies have proven that O. japonicus exhibits prominent therapeutic effects against angina pectoris, diabetes, chronic pharyngitis, and persistent cough (Peng et al. 2018). Incorporating O. japonicus into meal replacement powders can endow products with mild conditioning properties, enhance their nutritional and health benefits, and render them suitable for long-term dietary supplementation.

Dioscorea opposita Thunb., a classic medicinal and edible plant native to China, belongs to the Dioscoreaceae family (Guan et al. 2018). It is abundant in polysaccharides, saponins, pectin and cholesterol, possessing potentials in obesity prevention, hypoglycemia, hypolipidemia and cardiovascular disease mitigation (Zeng et al. 2022). Widely applied in meal replacement powder formulations, D. opposita can effectively improve the nutritional balance and edible safety of products.

Pulverization is a core processing technique for medicinal and edible meal replacement powders, critically affecting the release, bioavailability and functional performance of active ingredients (Li et al. 2025). Studies have confirmed that reduced particle size of herbal materials facilitates the dissolution and human absorption of active substances (Liu et al. 2025). (Jin et al. 2024) reported that ultrafine pulverization improves the rough texture of insoluble dietary fiber in white kidney bean hulls, promotes its fermentation to produce short-chain fatty acids, and thereby enriches intestinal flora diversity. (Wang et al. 2023) investigated the effects of different pulverization treatments on polysaccharide dissolution from alkali-extracted and water-extracted wheat bran. Traditional coarse pulverization results in large particle sizes, incomplete cell wall breakage, low active ingredient dissolution and insufficient functional activity (Duguma et al. 2023). In contrast, fine pulverization reduces particle size and increases specific surface area, which significantly enhances the dissolution rate, adsorption capacity and enzyme inhibitory activity of bioactive components, providing a reliable technical strategy for functional improvement of medicinal and edible meal replacement powders (Mei 2017).

Ophiopogon japonicus and Dioscorea opposita were used as main medicinal and edible raw materials in this study. Raw materials of Ophiopogon japonicus and Dioscorea opposita were pulverized to prepare meal replacement powders with different particle sizes. The effects of particle size on in vitro hypoglycemic and hypolipidemic activities were systematically evaluated via determining glucose dialysis retardation index, glucose adsorption capacity, α-amylase inhibition rate, cholesterol adsorption capacity, sodium cholate adsorption capacity and sodium cholate binding ability. The optimal pulverization parameters were finally determined. This work provides a theoretical basis for the development and industrial application of functional meal replacement powders from medicinal and edible materials.

METHOD

Experimental Raw Materials

Ophiopogon japonicus, purchased from Chengdu Qizi Miaoxiang Trading Co., Ltd.; *Dioscorea opposita*, locally produced in Li County; skimmed milk powder, purchased from Inner Mongolia Jinhetao Dairy Co., Ltd.; xylitol, purchased from Nanjing Ganzhiyuan Co., Ltd.

Experimental Methods

Preparation of *Ophiopogon japonicus* and *Dioscorea opposita* meal replacement powders with different particle sizes

The preparation processes of coarse powders of *Dioscorea opposita* and *Ophiopogon japonicus* are shown in **Error! Reference source not found.**, respectively. Fresh *Dioscorea opposita* was p eeled, sliced and fully steamed, then drained and dried in a thermostatic blast drying oven at 65 ℃ for 8 h. After cleaning and surface dewatering, *Ophiopogon japonicus* was dried under the same conditions. The cooled materials were coarsely pulverized separately. The obtained powders were sealed and stored in a desiccator for subsequent use.

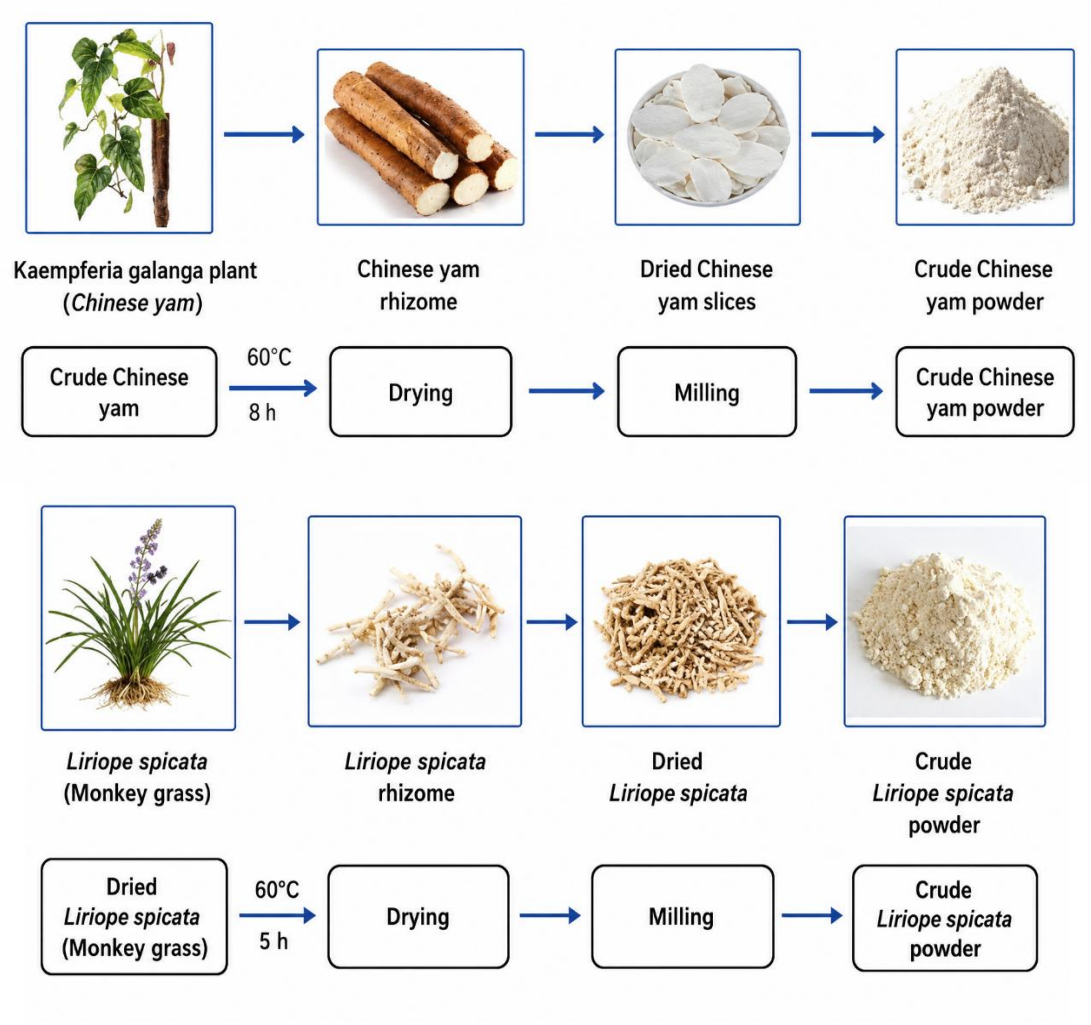

Figure 1. Preparation of Crude Ophiopogon Japonicus Powder

Coarse powders of *Dioscorea opposita* and *Ophiopogon japonicus* were separately sieved through standard sieves of 40, 60, 80, 100 and 120 mesh. Based on sensory evaluation score and caking rate as assessment indices in preliminary experiments, the optimal formula for the mixed meal replacement powder was determined by combining single-factor experiments and orthogonal tests. With a total mass of 20 g for yam and dwarf lilyturf powders, the mass ratios of *Ophiopogon japonicus* powder and *Dioscorea opposita* powder were 9.75% and 55.25%, respectively, corresponding to a mixing ratio of 1.5:8.5. In addition, the proportions of skimmed milk powder and xylitol were set at 25% and 10%. All ingredients were thoroughly blended to prepare five composite powder samples with different particle sizes. The prepared samples were hermetically stored in a desiccator for subsequent index determination.

Determination of In Vitro Hypoglycemic Activity

Determination of Glucose Dialysis Retardation Index

The method described by (Huang et al. 2013 ; Fu 2019) was adopted. Accurately weigh 0.5 g of sample, add 15 mL of 100 mmol/L glucose solution, mix thoroughly, and shake continuously for 1 h. Transfer the mixture to a dialysis bag with a molecular weight cutoff of 7000 and a length of 20 cm, and perform dialysis in deionized water at 37℃in a constant-temperature water bath shaker. A blank control group without sample was set up simultaneously. Each dialysis bag was placed in a beaker containing 200 mL of distilled water, and dialysis was performed with shaking at 37℃. At 20, 40, 60, and 80 min, 1.0 mL of dialysate was precisely collected. The glucose dialysis retardation index (GDRI) was calculated using the following formula:

$$\text{GDRI}\ (\%) = \left(1-\frac{\text{Glucose dialysis amount in sample cup}}{\text{Glucose dialysis amount in control cup}}\right) \times 100 \qquad (1)$$

Determination of Glucose Adsorption Capacity

The method described by (Zhang 2021 ; Daou & Zhang. 2012) was referenced. Accurately weigh 1.0 g of sample, add 100 mL of 100 mmol/L glucose solution (pH 7.0), mix thoroughly, and shake at 37℃ for 6 h. After shaking, transfer the mixture to a centrifuge tube, centrifuge at 3000 r/min for 20 min, and collect the supernatant. A blank control group without sample was set up simultaneously. The glucose adsorption capacity (GAC) was calculated using the following formula:

$$\text{GAC (mg/g)} = \frac{\text{Initial glucose content} - \text{Glucose content in supernatant}}{\text{Dry weight of sample}} \quad (2)$$

Determination of α-Amylase Inhibition Rate

The method described by (Lin 2024) was adopted. Accurately weigh 10.0 g of meal replacement powder sample, add 200 mL of deionized water, stir to dissolve, and reflux extract in a 100℃ water bath for 1 h. After cooling, centrifuge at 4000 r/min for 10 min. Pipette 500 μL of supernatant, add an equal volume of 1 U/mL α-amylase solution, and incubate at 37℃ for 10 min. Add 500 μL of 1% soluble starch solution, mix well, and continue incubating at constant temperature for 10 min. Add 1.0 mL of DNS chromogenic reagent to terminate the reaction, and heat in a boiling water bath for 5 min to completely inactivate the enzyme. After cooling, dilute to 10 mL and measure the absorbance at 520 nm. Acarbose was used as a positive control in the experiment. The α-amylase inhibition rate was calculated using the following formula:

$$\text{α-Amylase inhibition rate (\%)} = \left(1 - \frac{A_{\text{sample+enzyme}} - A_{\text{no-enzyme}}}{A_{\text{no-sample}}}\right) \times 100 \quad (3)$$

Where $A_{\text{sample+enzyme}}$, $A_{\text{no-enzyme}}$ and $A_{\text{no-sample}}$ represent the absorbance of the sample solution with enzyme, the absorbance of the sample solution without enzyme, and the absorbance of the solution without sample, respectively.

Determination of In Vitro Lipid-Lowering Activity

Determination of Cholesterol Adsorption Capacity

The method described by (Zhong et al. 2010) was referenced. Fresh commercially available eggs were selected, egg yolks were separated (egg whites discarded), and a yolk dilution was prepared by mixing egg yolk and distilled water at a volume ratio of 1:9. Transfer 50.0 g of the diluted yolk solution to two 250 mL conical flasks, add 1.0 g of sample to each flask, adjust the pH of the two systems to 2.0 and 7.0, respectively, and shake at 37℃ and 120 r/min for 2 h. After the reaction, transfer the mixture to a centrifuge tube, centrifuge at 4000 r/min for 20 min, and measure the absorbance of the supernatant at 550 nm. The cholesterol adsorption capacity (CAC) was calculated using the following formula:

$$\text{CAC(mg/g)} = \frac{\text{Cholesterol content before adsorptio} - \text{Cholesterol content after adsorption}}{\text{Mass of sample}} \times 100 \quad (4)$$

Determination of Sodium Cholate Adsorption Capacity

The method described by (Fu et al 2023 ; Feng 2016) was referenced. Take two 200 mL beakers, add 100 mL of 0.15 mol/L NaCl solution (containing 0.2 g sodium cholate) to each, and adjust the pH of both systems to 7.0. Add 2.0 g of test sample to each beaker, stir thoroughly with a glass rod, and shake at 37℃ and 120 r/min for 2 h. After the reaction, transfer the mixture to a centrifuge tube, centrifuge at 4000 r/min for 20 min, and pipette 1 mL of supernatant for sodium cholate content determination. The sodium cholate adsorption capacity (SCAC) was calculated using the following formula:

$$\text{SCAC(mg/g)} = \frac{\text{Sodium cholate content before adsorption-Sodium cholate content after adsorption}}{\text{Mass of sample}} \times 100 \quad (5)$$

Determination of In Vitro Simulated Sodium Cholate Binding Capacity

The method described by Sun Kaifeng (Sun 2019) was referenced. Weigh 4.0 g of sample into a 100 mL conical flask, accurately add 10 mL of amylase buffer, shake to mix, adjust the pH of the system to 6.9 with 1 mol/L NaOH solution, and shake in a water bath at 37℃ and 120 r/min for 5 min. Add 10 mL of 0.04 mol/L NaCl solution, mix thoroughly, adjust the pH to 2.0 with 1 mol/L HCl, add 600 μL of pepsin buffer, and continue shaking in a water bath at 37℃ and 120 r/min for 3 h. Add 10 mL of pancreatin-sodium cholate buffer, mix well, adjust the pH to 6.9 with 1 mol/L NaOH, add distilled water to bring the total mass of the system to 80 g, and shake at 37℃ and 120 r/min for 3 h. Accurately weigh 4.0 g of the above mixed digestive fluid into a dialysis bag, place the dialysis bag in a 50 mL beaker containing 20 mL of distilled water, seal, and shake at 37℃ and 90 r/min for 3 h to

simulate small intestinal absorption. After shaking, remove the dialysate, heat at 95℃ for 5 min to completely inactivate the enzyme, cool to room temperature, and use for sodium cholate content determination. The sodium cholate binding capacity (SCBC) of the sample was calculated using the following formula:

$$SCBC(\%)=\left(1-\frac{\text{Sodium cholate content in dialysate}}{\text{Sodium cholate content before dialysis}}\right)\times 100 \quad (6)$$

Statistical Analysis

All experiments were performed in triplicate, and results are expressed as mean ± standard deviation. Origin 2024 software was used for plotting, and SPSS 27.0 statistical software was employed for one-way analysis of variance (ANOVA) and inter-group significance testing.

RESULTS AND DISCUSSION

Analysis of In Vitro Hypoglycemic Activity

Analysis of Glucose Dialysis Retardation Index

As shown in Figure , the glucose dialysis capacity increased first and then decreased with the increase in crushing particle size. In the range of 80–100 mesh, the GDRI rose as crushing fineness increased. At dialysis times of 20, 40, 60, and 80 min, the GDRI reached maximum values at 100 mesh, at 56.42%, 53.25%, 49.85%, and 45.55%, respectively. This may be because, within the moderate crushing range, increasing the mesh number of raw materials reduces powder particle size, significantly increases surface area, accelerates the permeation and diffusion of glucose molecules, and thus gradually enhances glucose dialysis capacity (Wang et al. 2023). The index decreased at 100–120 mesh, possibly because excessive crushing relatively increases the proportion of insoluble dietary fiber, which forms a physical barrier to glucose molecules and traps them via a network structure, slowing their diffusion rate (Chang et al. 2016).

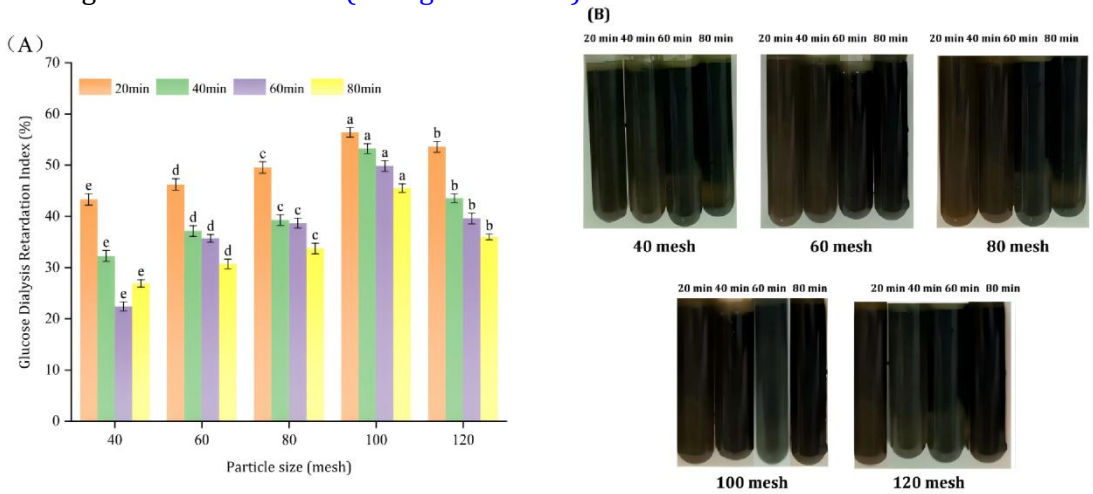

Figure 2. Effect of Crushing Particle Size on GDRI of Meal Replacement Powder (%)

For all mesh sizes, the glucose dialysis retardation index gradually decreased with prolonged dialysis time, reaching maximum values at the initial dialysis stage (20 min) of 43.30%, 46.25%, 49.56%, 56.43%, and 53.60%, respectively. This change may be attributed to the intact gel network structure formed by dietary fiber, polysaccharides, and other components in the meal replacement powder at the initial stage, which strongly encapsulates and adsorbs glucose, significantly slowing its dialysis rate (Feng et al 2016). As dialysis time extends, the encapsulated and adsorbed glucose is slowly released, and the glucose concentration inside and outside the system tends to balance, leading to a gradual decrease in the glucose dialysis retardation index over time (Jiang et al. 2026).

3.1.2 Analysis of Glucose Adsorption Capacity

As illustrated in Figure 3, the glucose adsorption capacity increased firstly and then decreased with the rise of crushing particle size. Within the range of 40–80 mesh, GAC slightly rose as particle size decreased, while no significant difference was observed among groups ($p>0.05$). When the crushing fineness reached 100 mesh, GAC increased significantly ($p<0.05$) and peaked at 167.73

mg/g. This variation is closely associated with the powder microstructure, hydration properties of dietary fiber, exposure of functional groups and glucose-binding capacity after ultrafine grinding (Niu et al 2022). Moderate grinding can preserve the structural integrity of dietary fiber and form pores with appropriate sizes, which effectively captures and binds glucose molecules. Accordingly, the adsorption performance is improved, and the sample exhibits favorable hypoglycemic potential (Zhang et al. 2023).

When the crushing fineness was further refined to 120 mesh, GAC slightly declined to 167.38 mg/g, with no statistical difference compared with the 100-mesh group ($p>0.05$). Excessive mechanical force would destroy the inherent micro-skeleton structure, resulting in ultra-fine and loose powder particles with oversized and uneven pores. In this case, it is difficult to construct a stable and dense gel network (Li et al. 2023). Meanwhile, intense mechanical treatment may inactivate partial active functional groups, reduce the binding efficiency toward glucose molecules, and eventually lead to a decrease in GAC (Guo et al. 2018).

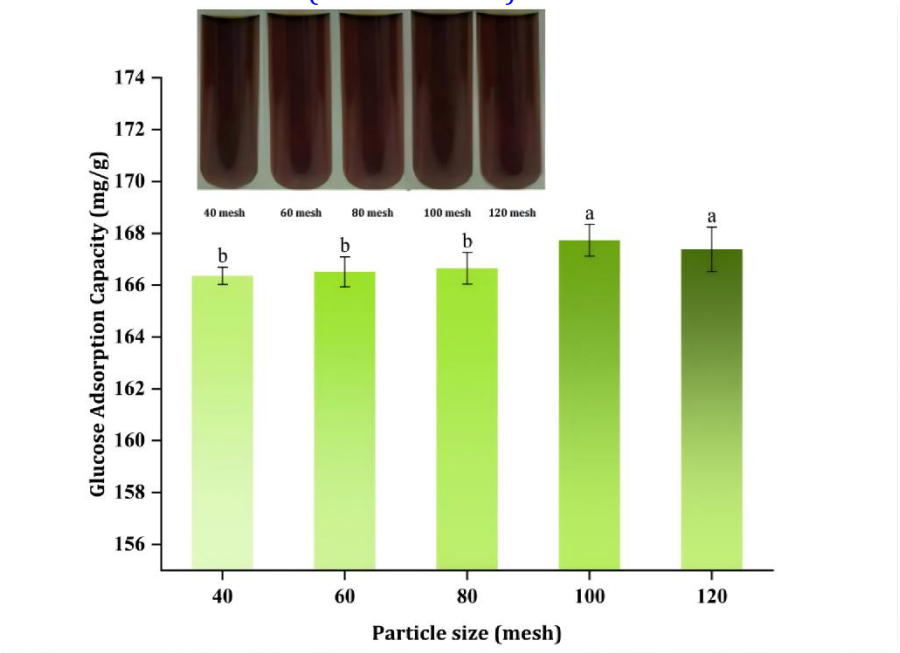

Figure 3. Effect of Crushing Particle Size on GAC of Meal Replacement Powder (mg/g)

Analysis of α-Amylase Inhibition Rate

As shown in Figure , all five meal replacement powder samples with different crushing fineness exhibited α-amylase inhibitory effects, with inhibition rates of 53.63%, 63.22%, 75.48%, 60.63%, and 43.60%, respectively, showing an overall trend of first increasing and then decreasing. The positive control acarbose had the highest α-amylase inhibition rate of 90.72%. Among the five samples, the 80 mesh powder showed the best inhibitory effect. This may be because gradual increase in crushing fineness optimizes powder surface area and internal pore structure, providing a larger contact area and reaction space for α-amylase and inhibitory active sites, thereby significantly enhancing α-amylase inhibition (Guo et al. 2024).

The α-amylase inhibitory effect gradually decreased at 80–120 mesh. This may be due to excessive particle refinement leading to structural compaction, significant reduction in internal pore size, and difficulty for α-amylase to enter particles and fully contact active sites, resulting in a sharp decrease in effective reaction area (Xu et al. 2024). In addition, excessive crushing may damage the structure of some active ingredients, and overly fine particles tend to agglomerate, further hindering effective binding between the enzyme and inhibitor and reducing α-amylase inhibition rate (Fu et al. 2025).

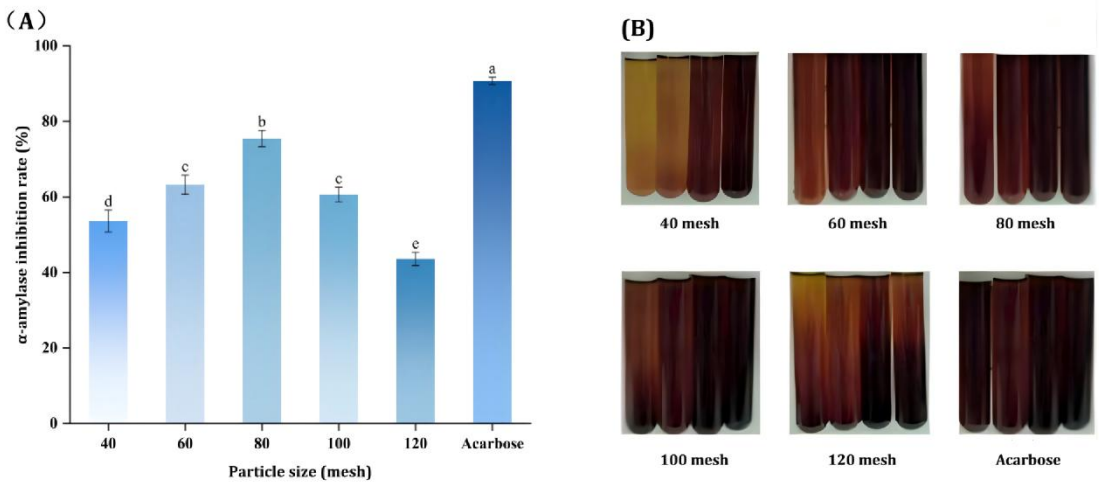

Figure 4. Effects of particle size on α-amylase inhibition rate of meal replacement powder (%)

Analysis of In Vitro Lipid-Lowering Activity

Analysis of Cholesterol Adsorption Capacity

As shown in Figure , cholesterol adsorption capacity of all samples was significantly higher at pH 7.0 than at pH 2.0. This may be because H^+ in acidic environments repels charges on soluble dietary fiber and cholesterol, hindering effective contact and binding between dietary fiber and cholesterol and making it difficult to form stable adsorption complexes, resulting in low cholesterol adsorption capacity (Benitez et al. 2019). As pH increases, carboxyl groups in soluble dietary fiber dissociate, repulsive forces weaken significantly, and electrostatic attraction, hydrogen bonding, and hydrophobic interactions promote tight binding between cholesterol and dietary fiber, leading to superior cholesterol binding properties (Li et al. 2024). This result reflects the actual environment of the human gastrointestinal tract, indicating that the meal replacement powder exhibits more stable cholesterol binding in the neutral intestinal environment.

In simulated intestinal fluid (pH 7.0), cholesterol adsorption capacity of all samples increased first and then decreased with decreasing powder particle size. It gradually increased in the range of 40–100 mesh, reaching a maximum value of 1.38 mg/g at 100 mesh. This may be because increased crushing fineness enlarges powder surface area, exposes more active sites and dietary fiber components, increases contact probability with cholesterol molecules, and gradually enhances adsorption capacity (Guo et al. 2016). Adsorption capacity decreased in the range of 100–120 mesh, possibly because excessive mechanical crushing destroys the original porous spatial structure of dietary fiber, reducing its ability to intercept and load cholesterol (Teng 2012). Thus, moderate crushing maximizes cholesterol adsorption capacity, while excessive crushing weakens adsorption effects.

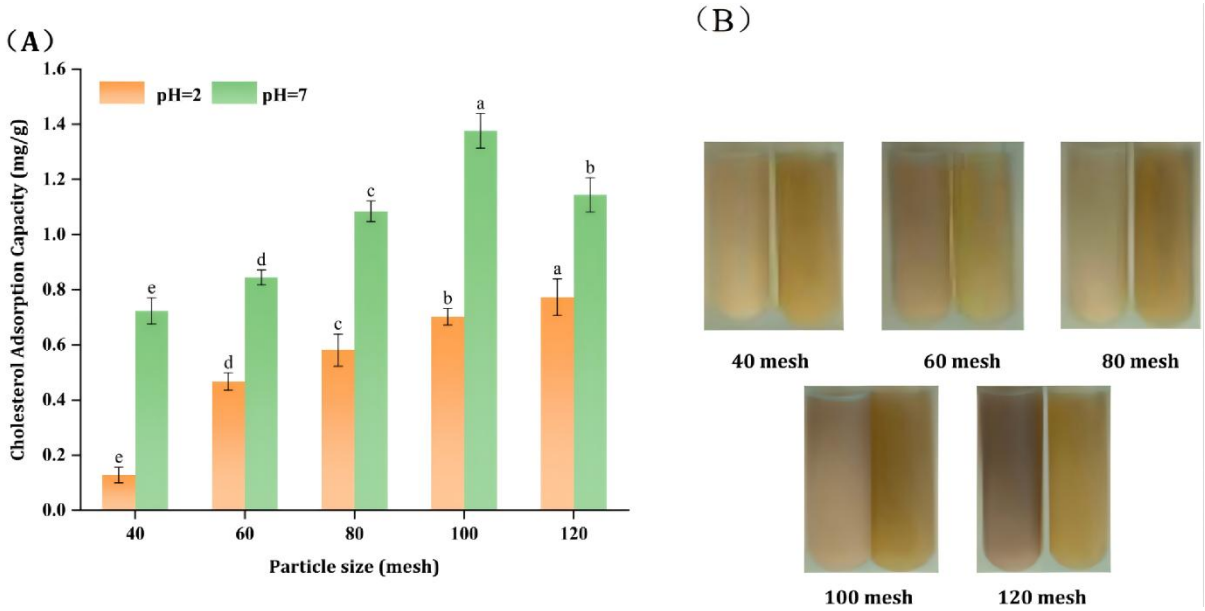

Figure 5. Effect of Crushing Particle Size on CAC of Meal Replacement Powder (mg/g)

Analysis of Sodium Cholate Adsorption Capacity

As shown in Figure , sodium cholate adsorption capacity increased first and then decreased with increasing mesh number, reaching an optimal value of 16.01 mg/g at 100 mesh. In the range of 40–100 mesh, sodium cholate adsorption capacity gradually increased. This may be because increased crushing fineness enlarges powder surface area, exposes more polar groups of dietary fiber, polysaccharides, and other components inside raw materials, and significantly increases soluble dietary fiber content (Hao 2023). Meanwhile, fine crushing disrupts the original spatial structure of raw materials, releases internal soluble dietary fiber, which swells upon water absorption to form a viscous gel network structure, thereby binding more sodium cholate (Huang et al. 2025).

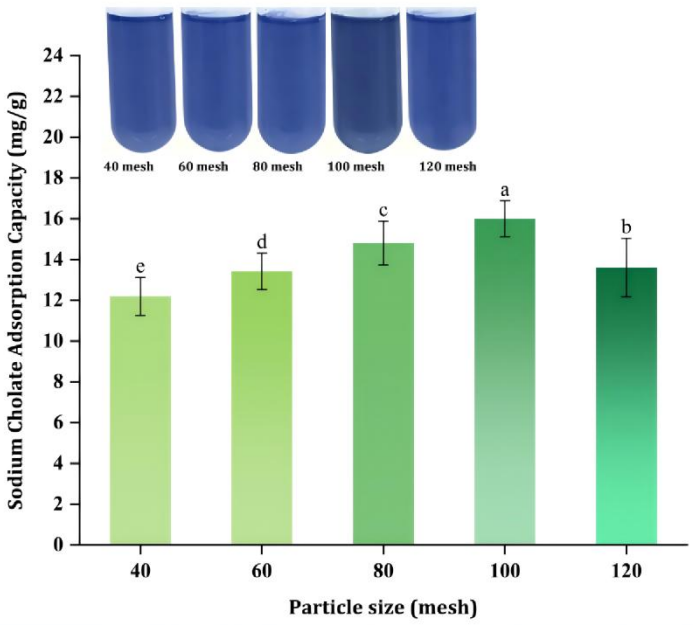

Figure 6. Effect of Crushing Particle Size on SCAC of Meal Replacement Powder (mg/g)

Sodium cholate adsorption capacity gradually decreased when the mesh number exceeded 100 mesh. Comparison with cholesterol adsorption capacity at pH 7.0 showed that both adsorption peaks occurred at 100 mesh, indicating that meal replacement powder prepared from 100-mesh crushed raw materials exhibits balanced and superior cholesterol and sodium cholate adsorption capacities in neutral environments, with more balanced lipid-lowering functions (Yang et al. 2024).

Analysis of In Vitro Simulated Sodium Cholate Binding Capacity

As shown in Figure , the sodium cholate binding rate of meal replacement powder prepared with different crushing particle sizes exhibited an overall trend of first increasing and then decreasing, reaching a maximum value of 69.41% at 100 mesh. Binding capacity gradually increased in the range of 40–100 mesh. This may be because moderate ultrafine crushing significantly increases particle surface area, fully exposes internal functional components, and provides more binding sites for sodium cholate molecules (Liu et al 2022). The 100-mesh powder has a large surface area, an uncompacted internal pore structure, and a relatively loose dietary fiber network structure, resulting in stronger interception and fixation of sodium cholate and a higher binding rate (Lin et al 2024).

Binding capacity gradually decreased when refined to 120 mesh. This may be because continuous particle refinement damages the internal micro-skeleton, causes excessive pore shrinkage or particle agglomeration leading to densification, hinders diffusion and penetration of sodium cholate molecules, and ultimately significantly reduces binding capacity (Tu et al. 2025). This trend is consistent with that of key in vitro hypoglycemic and lipid-lowering indicators of the meal replacement powder described above.

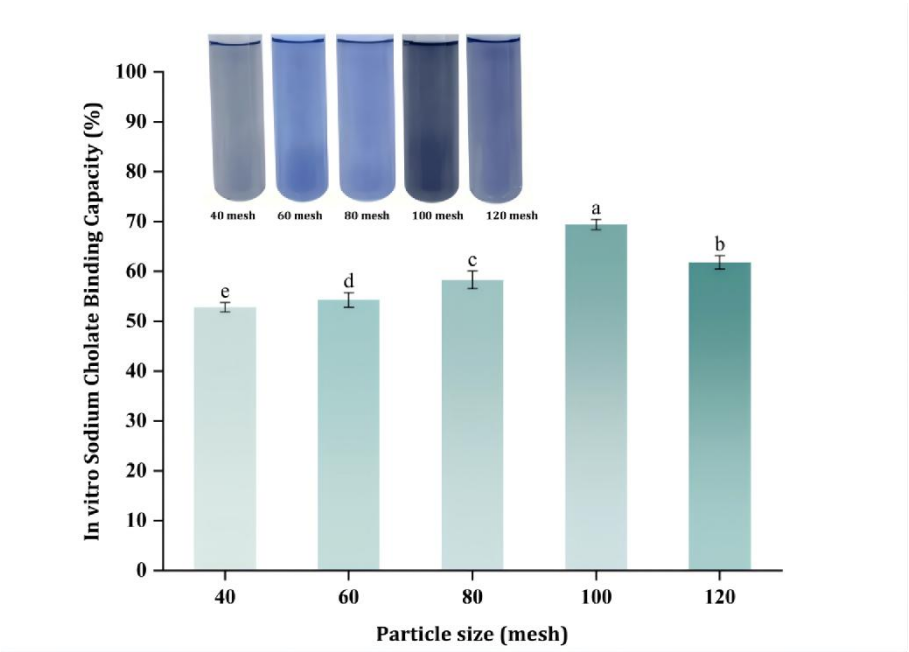

Figure 7. Effect of Crushing Particle Size on SCBC of Meal Replacement Powder (%)

CONCLUSION

This study focused on *Ophiopogon japonicus* and *Dioscorea opposita* compound meal replacement powder, and systematically investigated the effects of different pulverization particle sizes on its in vitro hypoglycemic and hypolipidemic activities. The results demonstrated that particle size exerted a certain regulatory effect on the functional activities of the meal replacement powder. All functional indicators exhibited a trend of first increasing and then decreasing as the particle size decreased, indicating the existence of an optimal particle size range rather than a simple "the smaller, the better" relationship. In terms of hypoglycemic properties, both the glucose dialysis retardation index and glucose adsorption capacity reached their maximum values at 100 mesh, while the highest α-amylase inhibition rate (75.95%) was observed at 80 mesh. Regarding hypolipidemic activities, the adsorption and binding capacities of the samples for cholesterol and sodium cholate were the highest at 100 mesh.

Overall, pulverization particle size influences key functions of the meal replacement powder, including glucose adsorption, α-amylase inhibition, cholesterol adsorption, and sodium cholate binding, by altering the specific surface area, pore structure, and physical state of dietary fiber, thereby determining its in vitro hypoglycemic and hypolipidemic effects. Therefore, selecting an appropriate pulverization mesh size (80 or 100 mesh) can significantly enhance the functional

activities of the meal replacement powder. The findings of this study provide a theoretical basis for the process optimization and industrial application of functional meal replacement powders derived from medicinal and edible homologous materials.

REFERENCES

Benitez, V., Rebollo-Hernanz, M., Hernanz, S., et al. (2019). Coffee parchment as a new dietary fiber ingredient: Functional and physiological characterization. *Food Research International*, *122*, 105–113. https://doi.org/10.1016/j.foodres.2019.03.063

Chang, S. M., Zhang, Y. X., & Tian, Y. L. (2016). Effect of supercritical CO2 on physicochemical properties of pear pomace insoluble dietary fiber. *Food Research and Development*, *37*(7), 5–7.

Cheng, J. M., Xue, F., Zhang, Y. Y., Ji, J., & Liu, T. S. (2023). Research status, key technologies and countermeasures of medicinal and edible homologous product development. *Journal of Nanjing University of Chinese Medicine*, *39*(9), 814–826. https://doi.org/10.14148/j.issn.1672-0482.2023.0814

Daou, C., & Zhang, H. (2012). Study on functional properties of physically modified dietary fibres derived from defatted rice bran. *Journal of Agricultural Science*, *4*(9), 85–97. https://doi.org/10.5539/jas.v4n9p85Duguma, H. T., Zhang, L. Y., Ofoedu, C. E., et al. (2023). Potentials of superfine grinding in quality modification of food powders. *CyTA - Journal of Food*, *21*(1), 530–541. https://doi.org/10.1080/19476337.2023.2210211

Feng, Y. B. (2016). Effect of ultrafine grinding on in vitro hypoglycemic and lipid-lowering activities of pine nut dietary fiber. *Food Science and Technology*, *37*(23), 342–346, 350. https://dx.doi.org/10.13386/j.issn1002-0306.2016.23.056

Fu, G. (2019). *Modification and functional properties of dietary fiber from red pine nut membrane coat* [Master's thesis, Yanbian University]. https://doi.org/10.1016/j.carres.2025.109558

Fu, H. Z., Deng, M., Zhang, M. W., et al. (2023). Process optimization and physicochemical functional properties of dietary fiber from kudzu residue modified by *Aspergillus niger*. *Scientia Agricultura Sinica*, *56*(12), 2380–2394. https://doi.org/10.3864/j.issn.0578-1752.230216

Fu, J. X., Chai, Z., Li, Y., & Pan, S. K. (2025). Effects of ultrafine grinding on physicochemical properties and hypoglycemic activity of mung bean powder. *Food Science and Technology*, *50*(8), 173–180. https://doi.org/10.3389/fnut.2023.1117385

Fu, W., & Chen, Y. (2025). Structural characterization and anti-fatigue activity of *Ganoderma lucidum* polysaccharides. *Food Science and Technology*, *50*(10), 241–250. https://doi.org/10.3390/foods13172665

Gao, M. J., Zhao, B. Q., Mo, Q. G., et al. (2023). Chemical constituents of *Poria cocos* and research progress on its regulation of glucose and lipid metabolism. *Journal of Hubei University of Science and Technology (Medical Edition)*, *37*(03), 272–276. https://doi.org/10.3389/fnut.2026.1774161

Guan, Q. Q., Zhang, W. L., Du, F. L., et al. (2018). Research progress on biological activity and mechanism of yam polysaccharides. *Food and Nutrition in China*, *24*(3), 11–14.

Guo, W., Shu, Y., & Yang, X. (2016). Tea dietary fiber improves serum and hepatic lipid profiles in mice fed a high cholesterol diet. *Plant Foods for Human Nutrition*, *71*, 145–150. https://doi.org/10.1007/s11130-016-0536-4

Guo, Z. W., Ma, P., Diao, J. J., et al. (2018). Physicochemical and adsorptive properties of ultrafine soybean hull insoluble dietary fiber. *Food Science*, *39*(5), 106–112. https://doi.org/10.7506/spkx1002-6630-201805017

Hao, R. X. (2023). *Study on the effect of ultrafine ground oat bran on instant noodle quality* [Master's thesis, Inner Mongolia Agricultural University].

Huang, D. D., Qian, H. F., Yuan, H. N., et al. (2013). Functional properties of dietary fiber from rice bran prepared by xylanase. *Food and Fermentation Industries*, *39*(12), 30–34.

Huang, S., Wang, Y. Y., Yang, X., et al. (2025). Effects of different treatments on physicochemical properties of bayberry pomace powder. *Food Industry*, *46*(1), 80–84.

Jiang, Z. X., Cai, Z. F., Dong, S. S., Hu, X. W., Chen, C., Zhang, C. M., Zhao, J., Liu, H. L., & Wu, Y. (2026). Chemical modification of *Rosa roxburghii* Tratt polysaccharides and analysis of their antioxidant

and hypoglycemic activities. *Science and Technology of Food Industry*, *47*(2), 94–103. http://dx.doi.org/10.13386/j.issn1002-0306.2025020006

Jin, S., Zhang, B., Gao, T., et al. (2024). Effects of particle size and bound phenolic insoluble dietary fiber on in vitro fermentation characteristics of white kidney bean hull. *Science and Technology of Food Industry*, *45*(1), 118–127. https://doi.org/10.13386/j.issn1002-0306.2023040250

Li, M., Sun, T., & Li, H. R. (2025). Application and optimization of ultrafine grinding technology in nutritional health food processing. *Modern Food*, *(12)*, 115–117.

Li, N., Guo, Q. Q., Xiao, J., et al. (2023). The effect of ball milling on the structure, physicochemical and functional properties of insoluble dietary fiber from three grain bran. *Food Research International*, *163*, Article 112263. https://doi.org/10.1016/j.foodres.2022.112263

Li, S. F., & Tian, 'X. Y. (2024). Effect of steam explosion on structure and properties of soluble dietary fiber from different varieties of rice bran. *Science and Technology of Food Industry*, Advance online publication. https://doi.org/10.13386/j.issn1002-0306.2023110126

Lin, X. X. (2024). *Study on the effect of crushing particle size on quality characteristics of multigrain meal replacement powder* [Master's thesis, Inner Mongolia Agricultural University].

Liu, C. Q., Ren, Y., & Zhang, Y. L. (2022). Research status and strategies for quality control of medicinal and edible homologous foods. *China Journal of Chinese Materia Medica*, *47*(14), 3963–3967. https://doi.org/10.19953/j.issn.1001-6910.2022.14.22

Liu, L., Xiang, Y. J., Wang, J. F., et al. (2025). Research progress on ultrafine grinding of Chinese herbal medicines and comprehensive utilization of Chinese medicine residues. *Chinese Herbal Medicines*, *56*(8), 2984–2994. https://doi.org/10.7501/j.issn.1001-6890.2025.08.028

Liu, Y., Ao, H. P., Zheng, J. X., et al. (2022). Improved functional properties of dietary fiber from *Rosa roxburghii* Tratt residue by steam explosion. *Journal of Food Processing and Preservation*, *46*, Article e16119. https://doi.org/10.1111/jfpp.16119

Lou, S. H., Sun, X. J., Li, D. D., et al. (2025). Effects of drying methods on total flavonoid content and antioxidant properties of hawthorn. *Science and Technology of Food Industry*, *46*(1), 121–129.

Mei, G. B. (2017). Application and development prospect of ultrafine grinding technology in fruit and vegetable powder production. *Modern Food*, *14*, 36–38.

Niu, X. X., Liang, L., Wang, N., et al. (2022). Effects of ultrafine grinding and different particle sizes on functional properties of potato residue. *Journal of the Chinese Cereals and Oils Association*, *37*(1), 37–45.

Peng, W., Ma, X., Wang, J., et al. (2018). Research progress on chemical constituents and pharmacological effects of *Ophiopogon japonicus*. *Chinese Herbal Medicines*, *49*(2), 477–488. https://doi.org/10.7501/j.issn.1001-6890.2018.02.028

Sun, B. G., & Mo, Y. J. (2026). Development trends of food industry and innovative application of medicinal and edible foods. *Journal of Food Science and Technology*, *44*(1), 1–6. https://doi.org/10.12301/spxb202600071

Sun, K. F. (2019). *Effect of microbial fermentation on hypoglycemic and lipid-lowering functional activities of black fungus* [Master's thesis, Northeast Forestry University].

Teng, S. (2012). *Effect of ultrafine grinding on physicochemical properties of sweet almond red skin and process optimization* [Master's thesis, Xinjiang Agricultural University].

Tu, W. C., Xiong, D. W., Zhang, D. F., et al. (2025). Effect of grinding degree on structure and functional properties of modified bagasse dietary fiber. *China Condiment*, *50*(12), 31–37, 51.

Wan, M. X., Yuan, J., Zhang, Y. X., et al. (2023). Research progress on pharmacological effects of *Ophiopogon japonicus* extract and its active ingredients. *Drug Evaluation Research*, *46*(8), 1819–1826. https://doi.org/10.7501/j.issn.1674-6376.2023.08.024

Wang, H., Wang, L. J., Yue, C. L. R., et al. (2023). Effects of ultrafine grinding pretreatment on physicochemical properties of alkali-extracted and water-extracted wheat bran polysaccharides. *Science and Technology of Food Industry*, *44*(22), 19–27. http://dx.doi.org/10.13386/j.issn1002-0306.2022100202

Wang, X., Zhang, X., & Zhang, D. (2023). Enhancement of cation exchange and glucose binding capacity, flavonoids release and antioxidant capacity of Tartary buckwheat powder with ultrafine grinding. *Frontiers in Nutrition*, *10*, Article 1276017. https://doi.org/10.3389/fnut.2023.1276017

Wang, X. D. (2023). Ideological origin, connotation and contemporary development of "medicinal and edible homology". *Journal of Nanjing University of Chinese Medicine*, *39*(9), 809–813. https://doi.org/10.14148/j.issn.1672-0482.2023.0809

Xu, B., Zhang, A., Zheng, Y., et al. (2024). Influences of superfine-grinding and enzymolysis separately assisted with carboxymethylation and acetylation on the in vitro hypoglycemic and antioxidant activities of oil palm kernel expeller fibre. *Food Chemistry*, *449*, Article 139192. https://doi.org/10.1016/j.foodchem.2024.139192

Yan, Y., Liang, X., Qin, B., Lian, S. M., Wang, B. Z., & Yin, G. (2024). Analysis of 15 organophosphorus pesticide residues in 9 medicinal and edible herbs and dietary risk assessment. *Contemporary Chemical Industry*, *53*(2), 500–504.

Yang, R. H., Ye, Y., Liu, W. T., et al. (2024). Modification of pea dietary fibre by superfine grinding assisted enzymatic modification: Structural, physicochemical, and functional properties. *International Journal of Biological Macromolecules*, *267*(Part 2), Article 131408. https://doi.org/10.1016/j.ijbiomac.2024.131408

Zeng, J. Y., Huang, J. Y., Li, P., et al. (2022). Research progress on processing and comprehensive utilization of yam. *Food Science and Technology*, *47*(4), 62–68.

Zhang, M. Y. (2021). *Modification and application of wheat bran dietary fiber and its prebiotic effect on lactic acid bacteria* [Master's thesis, Hefei University of Technology].

Zhang, Q., He, Y. J., Li, Q. Q., et al. (2023). Effects of ultrafine grinding on physicochemical and functional properties of lemon pomace. *Food Science and Technology*, *48*(8), 90–97. https://doi.org/10.1002/jsfa.10608

Zhong, X. Q., Hu, W. E., & Lin, L. C. (2010). Adsorption of oil, cholesterol, sodium cholate and nitrite ions by dietary fiber. *Science and Technology of Food Industry*, *31*(5), 134–136.

Zhou, L. Y., Gao, Y., Tang, J. F., Wu, Y., Wang, X. Y., Li, B., Yu, R., Sun, Y. D., & Zhu, M. J. (2025). Research progress on *Ophiopogon japonicus* and its herb pairs. *Chinese Archives of Traditional Chinese Medicine*, *43*(12), 103–108.